International Congress Motor Vehicles & Motors 2014

Kragujevac, October 9th-10th, 2014

MVM2014-045

Slobodan Popović[1]
Nenad Miljić[2], Marko Kitanović[3]

EFFECTIVE APPROACH TO ANALYTICAL, ANGLE RESOLVED SIMULATION OF PISTON–CYLINDER FRICTION IN IC ENGINES

ABSTRACT: Most frequently used approach to describe, model and analyse engine effective performance and mechanical losses is largely based on global, time/angle averaged empirical friction models. Importance of detailed, systematic approach to simulation of motor car and its real-world behaviour in terms of combustion efficiency and overall fuel consumption is greater than ever. Therefore, commonly employed empirical or semi-empirical approaches seem insufficient in terms of precision and capabilities for global optimisation of power train system which poses a need to invest more attention into comprehensive angle-resolved, analytical models. Such models have been already presented elsewhere, mainly based on fundamental friction theory of Stribeck, however, simplifications in both slider mechanism dynamic and combustion simulation influenced insufficient accuracy and reliability. In this paper, detailed Stribeck's theory based analytical approach has been employed to model friction in contact of piston ring assembly to cylinder (PRAC) and piston skirt to cylinder (PSC), as well. Gas pressure trace was measured and used to predict instantaneous indicated and effective torque based on engine 1DoF dynamic model and friction models presented in paper.

KEYWORDS: engine, friction model, instantaneous crankshaft speed

INTRODUCTION

Considering constantly growing importance of the analytical approach to the Internal Combustion Engine (ICE) design, virtual prototyping and combustion dynamics optimisation, highly sensitive and accurate simulation model of the engine is necessary to predict and evaluate fuel economy and overall performance in both stationary and transient operation. Cyclic nature of the combustion process taking place in engine cylinder(s) and crank slider mechanism dynamics are directly reflected in instantaneous engine torque, both indicated and effective one, which is further seen as an input to vehicle transmission, as a most common case, or to any other machine using an ICE as a prime mover. The information on highly dynamic nature of the ICE is, therefore, contained in the data obtained through angle based measurement of instantaneous engine torque and crank shaft angular speed. Being a highly dynamic and non-linear system, ICE could be presented and effectively simulated only by means of non-linear simulation models. Such a model can be applied as to provide a reliable prediction of crankshaft response to cycling nature of combustion process, both in terms of effective torque and angular velocity, or to evaluate and analyse combustion process through reverse approach based on measurement of instantaneous angular speed.

The ICE simulation model prediction capabilities largely depend on the correct and detailed approach to the modelling of mechanical losses. Such a model should cope effectively with complex and diverse phenomena related to energy dissipation in friction generated in contacts of adjacent engine components in relative motion (i.e.

[1] *Dr Slobodan Popović, Assistant Professor, Internal Combustion Engines Department, Faculty of Mechanical Engineering, University of Belgrade, Kraljice Marije 16, 11120 Belgrade 35, Serbia, spopovic@mas.bg.ac.rs*
[2] *Dr Nenad Miljić, Assistant Professor, Internal Combustion Engines Department, Faculty of Mechanical Engineering, University of Belgrade, Kraljice Marije 16, 11120 Belgrade 35, Serbia, nmiljic@mas.bg.ac.rs*
[3] *Marko Kitanović, M.Sc., Research Assistant, Internal Combustion Engines Department, Faculty of Mechanical Engineering, University of Belgrade, Kraljice Marije 16, 11120 Belgrade 35, Serbia, mkitanovic@mas.bg.ac.rs*

piston rings and skirt, bearings, cams, tappets, valve stems, gears) and to energy used to drive engine auxiliaries (i.e. coolant and lubricant circulation pumps, fuel supply, electrical generator).

The class of fully empirical, global, time-averaged models represent the simplest and most commonly used approach to this problem. Models proposed by Chen and Flynn [1], Yagi et al. [2] and Milington and Hartles [3] are good examples for this class of models, however, prediction capabilities are rather poor without proper model calibration. Component, semi-empirical, time-averaged models, such as that of Sandoval [4] or Arsie et al. [5], provide an engineer with simple, yet effective tool for evaluation of design parameters and their influences on mechanical losses. Obviously, the nature of mechanical losses differs largely and therefore, global, particularly fully empirical models provide satisfactory solution only in terms of modelling of BMEP and mean effective torque. Considered the modelling of engine dynamic response this approach seems insufficient, and different phenomena must be analysed and modelled using different approaches and techniques.

The friction processes represent a dynamic component of mechanical losses, which implies an angle-based approach to modelling. Quite opposite to that, the power used to drive engine auxiliaries is commonly regarded as a stady-state component and can be simulated by time averaged, global models. According to Taylor [6], the friction in Piston Ring Assembly–Cylinder (PRAC) contact dominates contributing the mechanical losses of an ICE by approximately 40–50%, following by Piston Skirt–Cylinder (PSC) contact friction with up to 25%. The distribution of other components is as follows: engine bearings 20–30%, valve train 7–15%, and auxiliaries with 20–25%. Considering these numbers, the friction originating in PRAC and PSC contacts are the most influential, and therefore, the special attention should be paid to this particular engineering problem. Investing a time and effort in development of fully analytical, dynamic, angle-resolved models based on fundamental lubrication theories is therefore, more than justified.

This work focuses mainly on the losses due to friction generated in piston–cylinder contact. The Piston Ring Assembly–Cylinder (PRAC) and Piston Skirt–Cylinder (PSC) contacts are analysed, modelled and presented separately in detail. Other phenomena, namely losses in crank and cam shaft bearings, valve train and auxiliaries are briefly presented as well in order to provide a full overview of the model structure. However, keen reader is highly advised to consult extensive literature for more detailed approach to these topics. Model verification based on comparison of simulated and measured engine crankshaft angular speed was presented in the final section.

ENGINE FRICTION MODEL STRUCTURE OVERVIEW

Piston Ring Assembly–Cylinder Friction sub model

The number of simulation models have been presented in literature in the past and used more or less effectively to evaluate diverse design and process parameters influences to dynamic components of mechanical losses in ICE. From theoretical standpoint of view, the most complete and comprehensive models covering the friction in PRAC is that based on solution of Reynolds equation. More details on this extensive numerical approach were overviewed by Taylor [6], Stanley [7] and Livanos [8,9]. In engineering applications, these models are hardly to be considered as a first choice, having in mind extensive and complex computational effort needed to provide an engineer with data necessary for engine design and overall performance evaluation. Far more interesting and promising seems the approach based on Stribeck's theory. This approach is widely used for a period of time and well documented by Ciulli [10], Guzzomi [11],[12], Taraza [13][14], Zweiri [15],[16], Rakopulos [17], Kouremenos [18], Thring [19] and Lin [19]. Although based on same theoretical principles, models referenced here differ in number of details such as engine class to which the model is adopted (ship propulsion [17][18]), interpretation of piston ring geometry [7],[13][14], or in number of empirical constants [10],[13][16]. Ciulli et al. [10] recognize mixed and hydrodynamic lubrication as predominant and suggested approach based on Stribeck's theory. Stribeck's number (duty parameter), in general form can be defined as follows [6,7,21,22]:

$$S = \frac{\eta \cdot |v|}{W} \tag{1}$$

where η is lubricant dynamic viscosity, v is instantaneous relative velocity and W normal specific load per unit length. Friction coefficient μ relies on simple relations based on duty parameter S and coefficients C and m which are to be identified for each specific case:

$$\mu = C \cdot S^m \tag{2}$$

The model incorporates a number of empirical constants necessary to calculate friction coefficient for two regimes of mixed and hydrodynamic lubrication which are supposed to be predominant in piston–cylinder contact:

$$\mu_{pr,i}(\alpha)=\begin{cases}\dfrac{C_1-C_2}{C_3}\cdot S_{pr,i}(\alpha)+C_2, & S_{pr,i}(\alpha)\le C_3\\ C_4\cdot\left(\sqrt{S_{pr,i}(\alpha)-\sqrt{C_3}}\right)+C_1 & S_{pr,i}(\alpha)>C_3\end{cases} \tag{3}$$

Coefficient C_3 has a physical background representing critical value of duty parameter S_{cr}. Other constants are engine design and geometry related and must be identified experimentally. According to Stanley [7] and Taraza [13], oil film formation and its thickness (OFT) are predominantly influenced by piston ring geometry, namely ring curvature, but almost independent of the ring axial thickness. The piston ring curvature parameter (PRCP) is defined as the ratio of the ring profile recess "*c*" at the ring edge to the height "*a*" of the parabolic profile. The PRCP is presented in Figure 1. The PRCP varies within the range of 0.03 to 0.15, with an optimal value of 0.06. It is also shown in [7] that lubrication conditions in PRAC contact, within the engine working cycle, change from boundary in the vicinity of both TDC and BDC, via mixed to fully developed hydrodynamic lubrication around each piston mid stroke. General behaviour of Oil Film Thickness (OFT) indicating such lubrication scheme is presented in Figure 2.

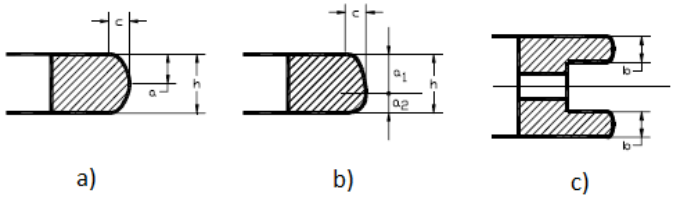

Figure 1 *Piston ring curvature: a) top compression ring; b) second ring; c) oil ring*

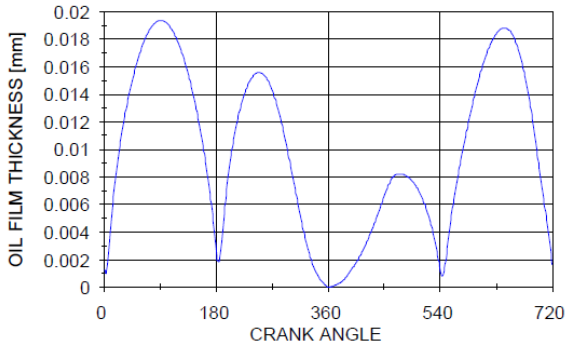

Figure 2 *OFT variation during an engine cycle for the top ring [13]*

According to these observations, separate angle-based sub-models can be set for each lubrication regime. Based on a Stribeck diagram presented in Figure 3, for regime of boundary lubrication, dry friction coefficient of the two rubbing metal surfaces μ_o can be used. Assuming that the values of S_{cr}, S_o and μ_o are known in advance (accessible from literature), the mixed lubrication friction coefficient can be retrieved from equation:

$$\ln\mu_{mix}=\frac{\ln\mu_{cr}-\ln\mu_o}{\ln S_{cr}-\ln S_o}\cdot\left(\ln S-\ln S_{cr}\right)+\ln\mu_{cr} \tag{4}$$

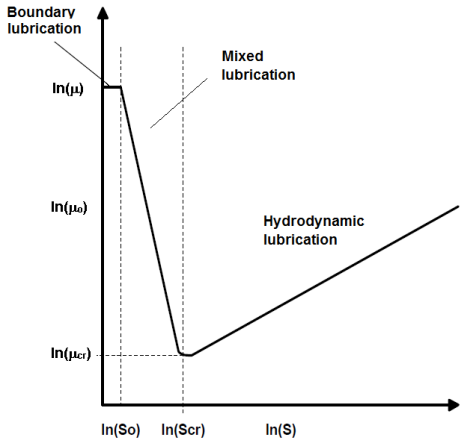

Figure 3 *The friction coefficient dependance on duty parameter (simplified Stribec's curve)*

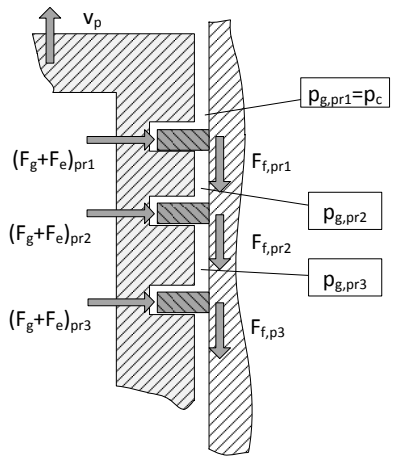

Figure 4 *Piston ring curvature: a) top compression ring; b) second ring; c) oil ring*

Summarizing previous equations, and applying general annotation to each piston ring of PRA, the model can be presented in angular domain as follows:

$$\mu_{pr,i}(\alpha)=\begin{cases}\mu_o & , \quad S_{pr,i}(\alpha)\le S_o \\ \mu_o\cdot\left(1-\dfrac{S_{pr,i}(\alpha)}{S_{pr,cr}}\right)+\mu_{cr}\cdot\dfrac{S_{pr,i}(\alpha)}{S_{pr,cr}} & , \quad S_{pr,i}(\alpha)\le S_{cr} \\ C_{pr}\cdot S_{pr,i}(\alpha)^{m_{pr}} & , \quad S_{pr,i}(\alpha)>S_{cr}\end{cases} \tag{5}$$

Recommended numerical values for constants μ_o, μ_{cr}, S_o, S_{cr}, C_{pr} and m_{pr} can be found in literature [7,13,14].

Duty parameter must be accommodated as to incorporate dependences on relevant PRA design and process parameters. From equation (1), one can retrieve expression for duty parameter for a given crank shaft angular position introducing $\eta(T_l)$ as lubricant dynamic viscosity dependant on lubricant temperature T_l, instantaneous piston velocity $v_p(\alpha)$ and piston ring normal load per unit length $W(\alpha)$. The most convenient way to express piston ring load per unit length W is to introduce the pressure acting on the piston ring $p_{pr,i}(\alpha)$ and corresponding piston ring axial thickness $a_{pr,i}$:.

$$S_{pr,i}(\alpha)=\frac{\eta(T_l)\cdot|v_p(\alpha)|}{W(\alpha)}=\frac{\eta(T_l)\cdot|v_p(\alpha)|}{p_{pr,i}(\alpha)\cdot a_{pr,i}} \tag{6}$$

Film thickness OFT, according to [17], can be expressed as a simple function of duty parameter and piston ring height.

$$OFT_{pr,1}=S_{pr,i}\cdot a_{pr,i} \tag{7}$$

The load acting on inner surface of each piston ring incorporates the effects of tangential force due to elastic nature of the piston ring and that of gas pressure coming from combustion chamber. The basic principle of piston ring friction mechanism is presented in Figure 4. According to [10] and [16], tangential force $F_{Tpr,i}$ and corresponding pressure $p_{Epr,i}$ are defined as follows:

$$F_{Tpr,i}=\frac{E_{pr}\cdot g_{o,i}\cdot h_{pr,i}\cdot\left(\dfrac{w_{pr,i}}{D}\right)^3}{14.14\cdot\left(1-\dfrac{w_{pr,i}}{D}\right)^3} \tag{8}$$

$$p_{Epr,i}=\frac{2\cdot F_{Tpr,i}}{D\cdot h_{pr,i}}=\frac{E_{pr}\cdot g_{o,i}\cdot\left(\dfrac{w_{pr,i}}{D}\right)^3}{7.07\cdot D\cdot\left(1-\dfrac{w_{pr,i}}{D}\right)^3} \tag{9}$$

Parameters are defined as follows:

- E_{pr} – Young's modulus of elasticity for piston ring material
- $g_{o,i}$ – Piston ring gap in open condition
- D – Nominal diameter (cylinder/piston)
- $w_{pr,i}$ – Piston ring radial thickness (piston ring width)
- $h_{pr,i}$ – Piston ring axial thickness (piston ring hight)

The resultant force acting on each piston ring incorporates a gas pressure which is particularly influential in the region of the compression piston ring. The expressions for resultant force $F_{pr,i}$, corresponding pressure $p_{pr,i}$ and friction force $F_{Fpr,i}$ are:

$$F_{pr,i}(\alpha)=\left[p_{Epr,i}+\left(p_{g,i}(\alpha)-p_o\right)\cdot\left(1-2\cdot\frac{w_{pr,i}}{D}\right)\right]\cdot\pi\cdot D\cdot h_{pr,i} \tag{10}$$

$$p_{pr,i}(\alpha)=p_{Epr,i}+\left(p_{g,i}(\alpha)-p_o\right)\cdot\left(1-2\cdot\frac{w_{pr,i}}{D}\right) \tag{11}$$

$$F_{Fpr,i}(\alpha) = \mu_{pr,i}(\alpha) \cdot F_{pr,i}(\alpha) \tag{12}$$

Gas pressure acting upon inner surface of each piston ring $p_{g,i}(\alpha)$ (Figure 4) is an unknown variable and can be determined by means of separate nonlinear thermodynamic model which can include gas leakage through each piston ring chamber and must be supported alternatively by in-cylinder pressure measurement or combustion process model. Such a complex approach has been presented by Dowson [6] and Wannatong [24]. However, much simpler, yet effective solution can be based on assumption that the pressure in the first piston ring chamber is almost equal to that in combustion chamber, while in the second and third piston ring chambers pressure is further reduced by a rate of approximately 50% and 90% respectively. This approach introduces a small angular phase shift in pressure traces compared to solution proposed by Dowson, particularly in the third piston ring chamber. However it can be neglected, having in mind a considerably small influence of the friction on the third piston ring.

Piston skirt–Cylinder Friction sub-model

Lubrication in Piston Skirt–Cylinder (PSC) contact is commonly assumed hydrodynamic. On that assumption, sub-model proposed for modelling friction in PRAC contact where duty number is higher than critical value will be used. Normal load is introduced through normal force F_N and piston skirt width w_{ps} which, depending on piston design features can incorporate also piston pin recesses.

$$\mu_{ps}(\alpha) = C_{ps} \cdot S_{ps}(\alpha)^{m_{ps}} = C_{ps} \cdot \left[\frac{\eta(T_l) \cdot |v_p(\alpha)|}{p_{ps}(\alpha) \cdot h_{ps}} \right]^{m_{ps}} = C_{ps} \cdot \left[\frac{\eta(T_l) \cdot |v_p(\alpha)| \cdot w_{ps}}{F_N(\varphi)} \right]^{m_{ps}} \tag{13}$$

Lubricant viscosity variations with temperature

Friction force in PRAC and PSC contacts as well in radial HD bearings, according to expressions (1)-(13) depend upon a lubricant dynamic viscosity which, in also depends upon lubricant temperature. This is of secondary importance if steady-state operation with stabilized lubricant temperature assumed, and viscosity can be determined from lubricant specifications. For full operating range this is insufficient, particularly if one takes into consideration a lubricant temperature rise due to the load and friction in surface contacts. According to Klaus [26], local increase in lubricant temperature of 50-60 K in radial HD bearings are highly expected.

The viscosity temperature relationship is commonly approximated by the ASTM, or simply MacCoull-Walther's equation [23], or MacCoull-Walther-Wright's equation [27]. More convenient approach is proposed by Manning based on Wright's equation [27]:

$$\log_{10}(\log_{10}(Z)) = A - B \cdot \log_{10}(T_l) \tag{17}$$

accompanied by equation for direct calculation of kinematic viscosity $\nu(T_l)$

$$\nu(T_l) = (Z - 0.7) - e^{f(Z)} \tag{18}$$

Function argument Z and complex polynomial function $f(Z)$ are well documented by Seeton [27], while coefficients A and B are determined by solving a system of equations given for two discrete values of viscosity and corresponding temperatures known from manufacturer's specification.

SIMULATION RESULTS

Piston Ring Assembly and Skirt Friction

The model components presented in previous section has been tested in order to check sensitivity and to provide basic conclusions necessary for further refinement and calibration. In-cylinder pressure data measured in firing engine were used to demonstrate models behaviour. The analysis was conducted for series-production PFI petrol engine DMB M202PB13 (technical data given in Table 1).

Table 1 *Main engine specification*

Description	Value
Engine manufacturer	DMB
Engine type	SI, MPI, M202PB13
Bore/Stroke	80.5/67.4 mm
No. of cylinders	4
Compression ratio	9.2 (+0.2/−0.1)
Max. power	52 kW @ 5800 min^{-1}
Cooling system	liquid
Fuel system	Port Injection

Table 2 *Operating points*

Engine Speed	Load (BMEP)
cca. 1810 min^{-1}	8.13 10^5 Pa
cca. 1810 min^{-1}	3.09 10^5 Pa
cca. 2810 min^{-1}	3.09 10^5 Pa

The first part of analysis was performed as to demonstrate basic influences of engine speed and load to OFT, friction coefficient and friction force in the piston ring–cylinder liner contact. The compression ring was chosen as a representative case, having in mind its dominant contribution in the overall friction in PRAC. Operating points chosen for this analysis were presented in Table 2. Figure 5 illustrates the dependency of the first piston ring (compression ring) OFT for 3 different operating points. OFT increases with an increase in engine speed and consequently piston speed. Provided the higher loads (higher BMEP) for a given constant engine speed, OFT decreases. This is expected because higher pressure in the first piston ring chamber (equal to the measured in-cylinder pressure) provides higher load to the back surface of the ring, and so, decreases the quantity of the lubricant in the contact. Both observations correspond with the results provided with more complex models based on Reynolds equation and experiments [6-9]. According to model, OFT riches minimum, i.e. zero values at each dead centre where piston changes direction and therefore, its speed is zero. This result cannot be considered entirely correct because it implies that lubricating oil vanishes from contact. The model, due to its simplicity, is not fully capable to predict minor phase shift due to transient hydrodynamic effects which is reported by Stenley [7]. However, model indicates correctly the regions where lubricating conditions are critical.

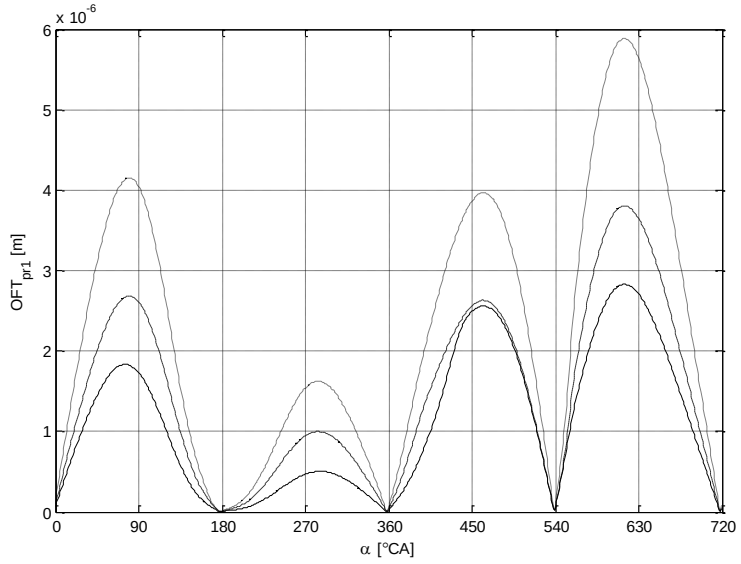

Figure 5 *Oil Film Thickness (OFT) for compression piston ring: cca. 30% load @ 1800 min^{-1} – dashed line; cca. 100% load @ 1800 min^{-1} – solid line; cca. 30% load @ 2800 min^{-1} – dotted line;*

The friction coefficient dependency on engine speed and load for the compression ring is presented in Figure 6. It follows the behaviour of OFT, and decrease in friction coefficient due to increased load, as well as lower values with increased speed are observed. Model indicates high gradients of friction coefficients in the regions close to each dead centre, which is expected because of the change in piston velocity.

The Figure 7 illustrates the friction force in PRAC. According to the observations presented for friction coefficient, intensive and sudden changes in friction force are indicated around each dead centre. However, the most dominant gradients are reported in the vicinity of the firing TDC, which is expected due to the effect of the rising pressure due to the combustion. The influence of piston speed is visible, but significantly smaller than that of the engine load. These results correspond well with basic findings reported by other authors [6-10,13,17-20]. Results are indicative, however further refinements for smooth transitions from mixed to boundary lubrication and *vice versa*, are needed.

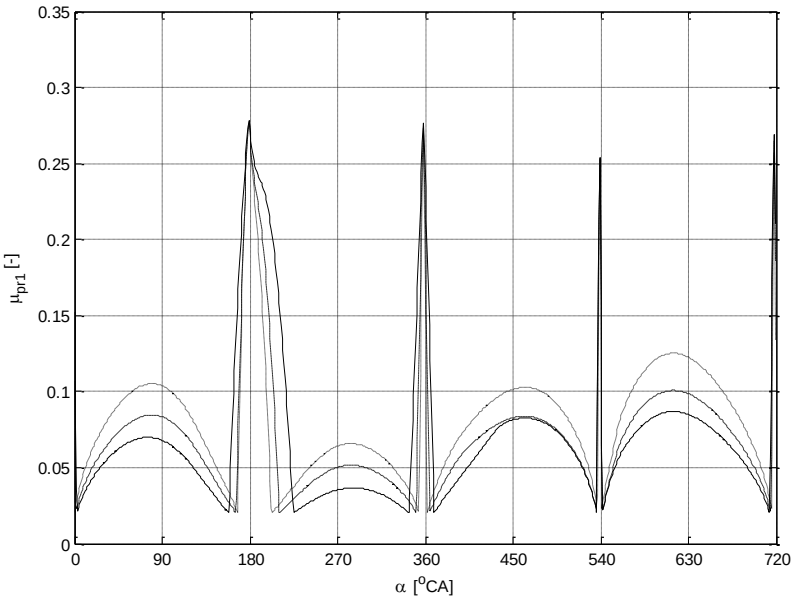

Figure 6 *Friction coefficient in PRAC (compression piston ring): cca. 30% load @ 1800 min^{-1} – dashed line; cca. 100% load @ 1800 min^{-1} – solid line; cca. 30% load @ 2800 min^{-1} – dotted line;*

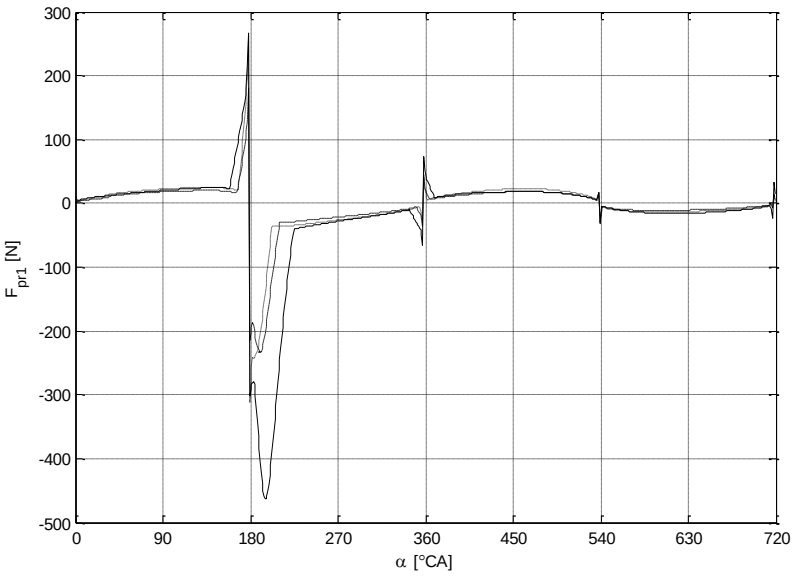

Figure 7 *Friction force in PRAC (compression ring): cca. 30% load @ 1800 min^{-1} – dashed line; cca. 100% load @ 1800 min^{-1} – solid line; cca. 30% load @ 2800 min^{-1} – dotted line;*

The influence of engine speed and load on friction force in PSC contact is presented in Figure 8. As expected, the increase in friction force is strongly related to the changes of normal force which pushes piston to the surface of the cylinder liner. The piston skirt friction force develops as normal force increases after the engine firing, therefore, angular phase shift in respect to the friction force in PRAC contact is clearly visible. The influence of engine load is visibly stronger than that of piston speed. The effect of piston skirt friction force is, however, of the marginal importance during exhaust and intake strokes, and for simplicity, can be neglected.

Total friction torque per cylinder, incorporating friction in PRAC and PSC contacts is presented in Figure 9. Basically, the model indicates that the friction due to normal force in PSC contact dominates. The influence of combustion around TDC is smaller due to the effect of crank slider mechanism dynamics. This diagram indicates that model provides solid information on basic both geometric and process parameters which influences friction in piston–liner assembly, and which can be regarded as an optimisation objective.

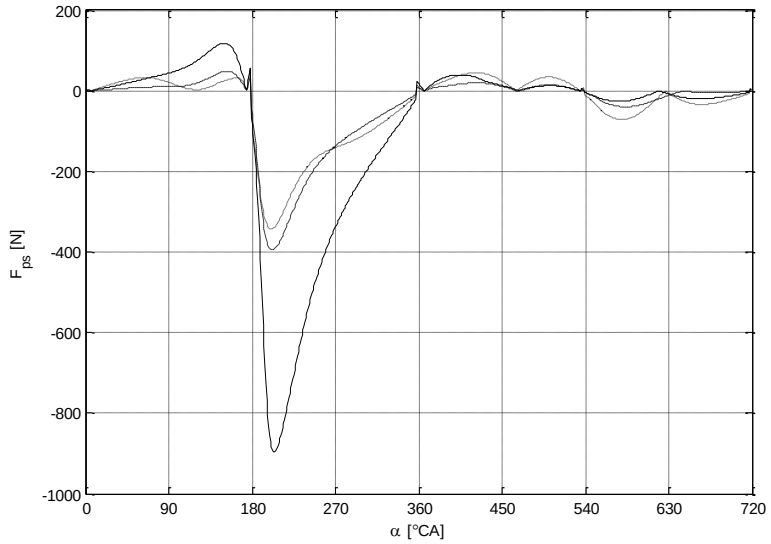

Figure 8 *Friction force in PSC: cca. 30% load @ 1800 min^{-1} – dashed line; cca. 100% load @ 1800 min^{-1} – solid line; cca. 30% load @ 2800 min^{-1} – dotted line;*

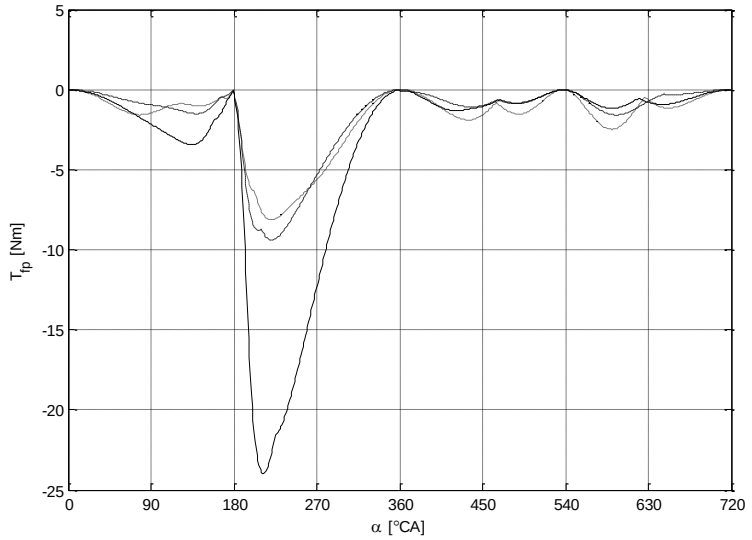

Figure 9 *Total friction torque in PRAC and PSC contact per cylinder: cca. 30% load @ 1800 min^{-1} – dashed line; cca. 100% load @ 1800 min^{-1} – solid line; cca. 30% load @ 2800 min^{-1} – dotted line;*

MODEL VERIFICATION

Piston-cylinder liner friction model was used to compare simulated and measured values of instantaneous crankshaft angular speed. As an input to simulation model, in-cylinder pressure was provided experimentally. However, in order to provide correct simulation, an extension to friction losses in piston–cylinder contact model must be provided as to encounter friction in bearings, valve train and power for engine auxiliaries.

Friction in bearings

Engine bearings (crank and cam shafts) are exposed to variable loading which reflects dynamic nature of the combustion process and geometric features of the crank slide and cam-tappet mechanisms. Being responsible for approximately 20% of total losses, special attention must be paid to the modelling of phenomena related to hydrodynamic lubrication in radial bearings. In order to provide effective and accurate calculation, model must incorporate gas pressure force as an input, friction force in piston–cylinder contact, inertia forces acting on both rotating and reciprocating masses which, through iterative approach can lead to a bearing loading force determination. Resultant force acting in connecting rod bearing is determined through clear approach. However, resultant force in main bearings of a multi-cylinder engine which is the most often case, poses a number of issues related to load distribution along the crankshaft which is generally considered as statically underdetermined

structure. According to [25], reactions on bearings situated outside the crank on which a force is applied are low due to the shaft stiffness. Accordingly, crankshaft/camshaft can be assumed as a structure consisting of successive sections (cranks or cams, depending on the case) transmitting only torque, while the resulting radial load in main bearings can be approximated as a sum of load reactions in adjacent cranks/cams.

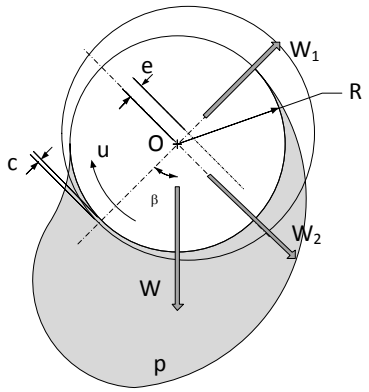

Figure 10 *Pressure profile and load distribution in radial HD bearing*

The mobility method proposed by Booker [6], which is based on OFT determination, provides quite satisfactory results in terms of computational effort and accuracy, and will be deployed here as well. Complete, general, theoretical approach is well documented by Stachowiak [23]. For the purpose of current study, this method will be shortly reviewed with the emphasis on basic components and necessary corrections which must be applied for short dynamically loaded bearing. In order to establish the relationship between total bearing load, which comes from engine crank slide mechanism dynamic calculation model, and basic geometry of a bearing, expression for instantaneous load capacity of the bearing *W* will be used based on general analytical approach [23].

$$W = \sqrt{W_1^2 + W_2^2} = \frac{u \cdot \eta(T_L) \cdot \varepsilon \cdot L^3}{c^2 \cdot \left(1-\varepsilon^2\right)^2} \cdot \frac{\pi}{4} \cdot \sqrt{\left(\frac{16}{\pi^2} - 1\right) \cdot \varepsilon^2 + 1} \tag{14}$$

The expression corresponds to the bearing disposition presented in Figure 10. Parameters are defined as follows: u represents the instantaneous journal velocity relative to bearing, c is the bearing clearance, ε is the relative eccentricity of the journal in the bearing (e/c). The attitude angle β between the load line and the line of centres Figure 10) can be determined directly from the load components W_1 and W_2 from the following relation:

$$\beta = \tan^{-1}\left(-\frac{W_2}{W_1}\right) = \tan^{-1}\left(\frac{\pi}{4} \cdot \frac{\sqrt{1-\varepsilon^2}}{\varepsilon}\right) \tag{15}$$

Considering engine shaft radial bearing a short one, friction force F_{Fb} can be determined from model proposed by Ocvirk [13][14] [23].

$$F_{F,b} = \left[\frac{2 \cdot \pi \cdot \eta(T_l) \cdot u \cdot L \cdot R}{c \cdot \sqrt{1-\varepsilon^2}}\right]_1 + \left[\frac{e \cdot W}{2 \cdot R} \cdot \sin\beta\right]_2 + \left[\frac{v \cdot W}{u} \cdot \cos\gamma\right]_3 \tag{16}$$

The friction force equation introduces three components, the first of which is dominant and represents the influence of shearing force of the lubricant film, while the second one simulates the contribution of the torque due to the eccentric load. The third term represents a correction for dissipation due to the journal movement which can be neglected for quasi-static conditions. The model considered at this point is a quasi-steady-state model assuming established equilibrium values for the unknown relative eccentricity ε and attitude angle β for every direction and magnitude of the load. These values are determined iteratively using formulation for Sommerfeld Number. More details on this approach can be found in selected literature [21] and [23]

Friction in valve train

Mechanical losses in valve train were predicted by means of simplified time averaged model presented by Sandoval et al. [4]. The model incorporates exclusively those terms relevant for design of valve train system of engine used in experiment. The model provides FMEP, which can be effortlessly converted in torque and power. The model is presented as a single line equation:

$$FMEP_{vts} \approx C_{ff} \cdot \left(1+\frac{500}{n}\right) \cdot \frac{i_v}{s \cdot i_c} + C_{oh} \cdot \sqrt{\frac{\eta(T_l)}{\eta(T_{l,o})}} \cdot \left(\frac{h_{v,\max}{}^{1.5} \cdot n^{0.5} i_v}{D \cdot s \cdot i_c}\right) + C_b \cdot \sqrt{\frac{\eta(T_l)}{\eta(T_{l,o})}} \cdot \frac{n \cdot i_b}{D^2 \cdot s \cdot i_c} \quad (19)$$

Where i_v is a number of valves, i_c number of cylinders, i_b number of bearings s and D piston stroke and bore respectively, and $h_{v,max}$ valve lift. The first term includes the effect of mixed lubrication for flat follower and the second one evaluates hydrodynamic friction in tappet–liner and valve–guide contacts. The last term evaluates friction in camshaft bearings. Other terms related to cam rollers and seals are neglected. Constants C_{ff}, C_{oh} and C_b can be found in literature [4].

Mechanical losses in engine auxiliaries

Energy used to provide coolant circulation depends on coolant pressure, coolant flow rate and hydraulic resistance in radiator and passages. The necessary flow rate depends on engine operation point, however can be estimated based on circulation pump outlet pressure, its speed and efficiency. The outlet pressure is proportional to the square of the flow rate, which is also proportional to the speed of the pump. The power is approximated as follows:

$$P_{pc} \approx n_{pc}{}^3 = \left(k_{pc} \cdot n\right)^3 \quad (19)$$

and, assuming that coolant circulation pump absorbs approximately 1% of engine nominal power $P_{e,max}$, relation can be recomposed as to incorporate ratio of instant engine speed to its nominal value n_{max}:

$$P_{pc}(n) = P_{pc,\max} \cdot \left(\frac{n}{n_{\max}}\right)^3 = 0.01 \cdot P_{e,\max} \cdot \left(\frac{n}{n_{\max}}\right)^3 \quad (20)$$

Engine lubrication system absorbs mechanical power from crankshaft which can be for common gear type pump determined from lubrication system pressure p_l and known pump design parameters namely, nominal diameter D_{po}, teeth height h_t, gear height h_p , pump to engine speed ratio k_{pl} and pump volumetric and mechanical efficiency $\eta_{pl,v}$ and $\eta_{pl,v}$, respectively:

$$P_{pl}(n, p_L) = \frac{Q_l(n) \cdot p_l}{\eta_{pl,m}} = D_{po} \cdot h_t \cdot h_p \cdot k_{pl} \cdot \frac{\eta_{pl,v}}{\eta_{pl,m}} \quad (21)$$

Assuming equal values for both volumetric and mechanical efficiencies $\eta_{pl,v}$ and $\eta_{pl,v}$, previous expression becomes dependant on known parameters, retaining uncertainty of less than 0.2%.

Experimental verification

In this work, simplified 1-DoF dynamic engine model is applied to simulate crankshaft instantaneous angular speed. Engine-dynamometer dynamic system is presented in Figure 11. Engine mass moment of inertia J_E is assumed as a function of both mass and position of slider mechanism components in respect to shaft angle position. Engine inertia and its first derivative in respect of crank angle are calculated by means of dynamically equivalent model, while inertia of flywheel J_{FW}, connecting shaft J_S and dynamometer J_D are known constants obtained from manufacturing specification. Assuming crank and connecting shafts rigid [1][3], torque balance equation for engine-dynamometer system arises from kinetic energy equation (Newton's principle):

$$\left[J_E(\alpha) + J_{FW} + JS + J_D\right] \cdot \ddot{\alpha}(\alpha) + \frac{1}{2} \cdot \frac{dJ_E(\alpha)}{d\alpha} \cdot \dot{\alpha}(\alpha)^2 = T_G(\alpha) - T_F(\alpha) - T_L \quad (21)$$

Gas-pressure torque contributions from individual cylinders are denoted by term T_G while T_L is the measured load torque. The term T_F denotes the sum of torques from friction and mechanical losses in engine moving components and auxiliaries. In this analysis, in-cylinder pressure measured in 2nd cylinder, which is regarded as a master cylinder, was copied and phase shifted as to provide gas pressure torque T_G for an engine as a system. The term T_F was predicted by means of hybrid model (combination of angle-based and time-averaged components) presented in this work.

The instantaneous crankshaft angular speed was measured at power take-off (PTO) by means of flywheel gear as an incremental disc. The experimental results are presented in Figure 12 for three loads, BMEP 8.2 10^5 Pa, 6.04 10^5Pa and 3.16 10^5Pa at engine speed of approx. n=2300 min^{-1}. The measured signal was filtered, averaged on an

ensemble of 50 consecutive cycles, and smoothed using cubic approximation spline in order to retain smooth second order derivative (dash-dot line, Figure 12). The signal was corrected for flywheel radial run-out (dashed line, Figure 12). The simulation results were presented in solid line.

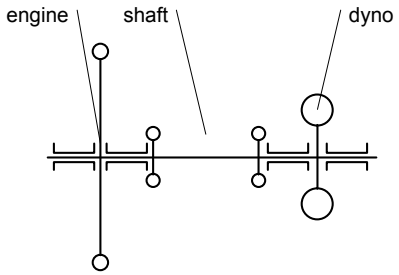

Figure 11 Reduced, equivalent 1-DoF Engine dynamic model

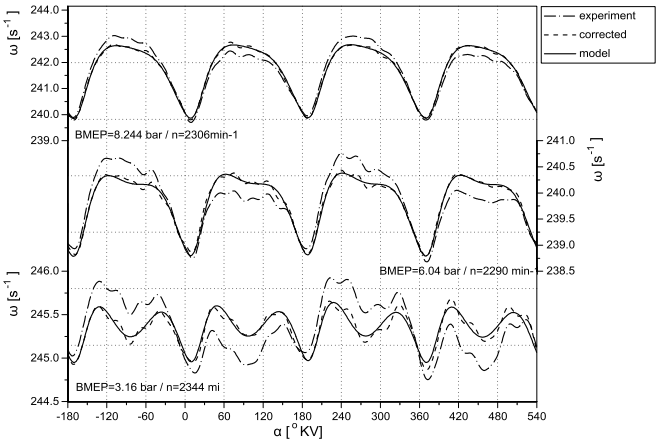

Figure 12 *Instantaneous crankshaft angular speed n=2300 min^{-1}*

The model for simulation of friction losses in PRAC and PSC contacts provided solid values for prediction of instantaneous crankshaft angular speed. The influence of mass inertia torques dominates over gas pressure torques at the low BMEP operating point. Here, uncertainties in engine friction and dynamic model become significant. The results improve at higher loads where gas pressure torque increases. Although the basic approach in friction modelling presented in this work is analytical and based on fundamental theories, it is still strongly affected by a number of design and empirical constants which must be carefully identified. In spite of that the simulation was performed using model set up based on numerical values accessible from literature, and having in mind simplifications implemented in model of engine crank slider mechanism dynamics and friction losses, the results are correct, follow the trends and provide solid prediction of engine dynamic behaviour in angle based presentations. Based on analysis in previous section, model can provide valuable information for process and design optimisation.

CONCLUSIONS

Simplified, angle-based approach to modelling of friction in Piston Ring Assembly – Cylinder contact and Piston Skirt – Cylinder contact were presented. The models were used to analyse the influence of engine speed and load to friction phenomena in piston – cylinder liner contact. The model provides generally good results in terms of global trends which were reported by other authors and based on both complex modelling and experimental verification.

The model was tested against instantaneous angular crankshaft speed and compared to values obtained experimentally. The model was supplemented by angle-based friction model in HD bearings, and time-averaged models for friction in valve train system and for power consumed by engine auxiliaries.

The model verification indicates solid prediction capabilities. Uncertainties in friction models exist, and empirical constants which cannot be avoided require careful identification. Procedure presented in this work, proved sufficiently robust and sensitive and provided improved in terms of friction coefficient identification could be used effectively for prediction of engine performance in dynamic operation.

ACKNOWLEDGMENTS

The authors would like to acknowledge the technical support of IC Engine Department Research Lab at the Faculty of Mech. Engineering, University of Belgrade and financial support of the Ministry of Education and Science of Republic of Serbia which, within the research projects NPEE-290025, TR-14074 and TR-35042

REFERENCES

[1] Chen, S. X., Moskwa, J. J.: “Application of Nonlinear Sliding-Mode Observers for Cylinder Pressure Reconstruction”, Control Engineering Practice. 5 (1997).
[2] Yagi, S et al.: “Estimate of Total Engine Loss and Engine Output in Four Stroke S.I. Engines”, SAE Technical Papers. (1991) SAE-910347.
[3] Filipi, Z. S., Assanis, D. N.: “A Nonlinear, Transient, Single-Cylinder Diesel Engine Simulation for Predictions of Instantaneous Engine Speed and Torque”, Journal of Engineering for Gas Turbines and Power. 123 (2001) 951-959.
[4] Sandoval, D., Heywood, J.: “An Improved Friction Model for Spark-Ignition Engines”, SAE Technical Papers. (2003) SAE 2003-01-0725.
[5] Arsie, I. et al.: “Development and Validation of a Model for Mechanical Efficiency in a Spark Ignition Engine”, SAE Technical Papers. (1999) SAE 1999-01-0905.
[6] Taylor, C. M.: “Engine Tribology”, Elsvier Science Publishers, 1993.
[7] Stanley, R. et al.: “A Simplified Friction Model of the Piston Ring Assembly”, SAE Technical Papers. (1999) SAE 1999-01-0974.
[8] Livanos, G. A., Kyrtatos, N. P.: “Friction model of a marine diesel engine piston assembly”, Tribology International. 40 (2007) 1441-1453.
[9] Livanos, G. A., Kyrtatos, N. P.: “Friction model of a marine diesel engine piston assembly”, Tribology International. 40 (2007) 1441-1453.
[10] Ciulli, E., Rizzoni, G., Dawson, J.: “Numerical and Experimental Study of Friction on a Single Cylinder CFR Engine”, SAE Technical Papers. (1996) SAE 960357.
[11] Guzzomi, A. L. Hesterman, D. C. Stone, B. J.: “The effect of piston friction on engine block dynamics”, Proceedings of the Institution of Mechanical Engineers, Part K: Journal of Multi-body Dynamics. 221 (2007) 277-289.
[12] Guzzomi, A. L. Hesterman, D. C. Stone, B. J.: “Variable inertia effects of an engine including piston friction and a crank or gudgeon pin offset”, Proceedings of the Institution of Mechanical Engineers, Part D: Journal of Automobile Engineering. 222 (2008) 397-414.
[13] Taraza, D., Henein, N., Bryzik, W.: “Friction Losses in Multi-Cylinder Diesel Engines”, SAE Technical Papers. SAE-2000-0 (2000) SAE 2000-01-0921.
[14] Taraza, D., Henein, N., Ceausu, R., Bryzik, W.: “Complex Diesel Engine Simulation with Focus on Transient Operation”, Energy & Fuels. 22 (2008) 1411-1417.
[15] Zweiri, Z. H., Whidborne, J. F., Seneviratne, L. D.: “Detailed analytical model of a single-cylinder diesel engine in the crank angle domain”, Proceedings of the Institution of Mechanical Engineers, Part D: Journal of Automobile Engineering. 215 (2001) 1197-1216.
[16] Zweiri, Z. H., Whidborne, J. F., Seneviratne, L. D.: “Instantaneous friction components model for transient engine operation”, Proceedings of the Institution of Mechanical Engineers, Part D: Journal of Automobile Engineering. 214 (2000) 809-824.
[17] Rakopoulos, C., et al.: “Application and Evaluation of a Detailed Friction Model on a DI Diesel Engine with Extremely High Peak Combustion Pressures”, SAE Technical Papers. (2002) SAE 2002-01-0068.
[18] Kouremenos, D. et al.: “Development of a Detailed Friction Model to Predict Mechanical Losses at Elevated Maximum Combustion Pressures”, SAE Technical Papers. (2001) SAE 2001-01-0333.
[19] Thring, R.: Engine Friction Modeling, SAE Technical Papers. (1992) SAE 920482.
[20] Lin, S.-S., Patterson, D. J.: “Piston-Ring Assembly Friction Modeling by Similarity Analysis”, SAE Technical Papers. (1993) SAE 930749.
[21] Popović, S. J.: “Research and Development of instantaneous crankshaft angular speed based method for engine combustion analysis”, PhD Thessis, University of Belgrade, 2013.
[22] Stolarski, T. A.: “Tribology in Machine Design”, Butterworth-Heinemann, Oxford, England, 2000.
[23] Stachowiak, G. W., Batchelor, A. W. : “Engineering Tribology”, Butterworth-Heinemann, Elsevier Inc., 2006.
[24] Wannatong, K.: “Simulation algorithm for piston ring dynamics”, Simulation Modelling Practice and Theory. 16 (2008) 127-146.
[25] Hafner, K. E., Maass, H.: “Theorie der Triebwerksschwingungen der Verbrennungskraftmaschine” Band 1-4, Springer-Verlag Wien/VEB Verlag Technik, Berlin, 1984.
[26] Klaus, E. E. , Tewksbury, E. J.: “Lubricants and Their Application”, CRC Handbook of Lubrication Theory and Practice of Tribology, Volume II: Theory and Design,, CRC Press, 1988.
[27] Seeton, C. J.: “Viscosity–temperature correlation for liquids, Tribology Letters. 22 (2006) 67-78.